LA-4775-MS

Space- and Time-Dependent Slowing Down in Heavy Media

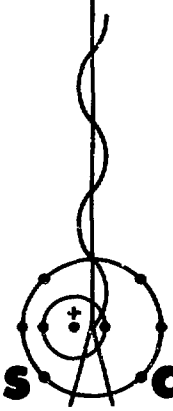

los alamos
scientific laboratory
of the University of California
LOS ALAMOS, NEW MEXICO 87544

UNITED STATES
ATOMIC ENERGY COMMISSION
CONTRACT W-7405-ENG. 36

Printed in the United States of America. Available from
National Technical Information Service
U. S. Department of Commerce
5285 Port Royal Road
Springfield, Virginia 22151
Price: Printed Copy $3.00; Microfiche $0.95

LA-4775-MS

UC-15

ISSUED: January 1972

los alamos
scientific laboratory
of the University of California
LOS ALAMOS, NEW MEXICO 87544

Space- and Time-Dependent Slowing Down in Heavy Media

by

C. R. Weisbin
R. A. Forster
D. B. Smith
N. Corngold*

*Los Alamos Scientific Laboratory Consultant. Present address, California Institute of Technology, Pasadena, CA 91109.

SPACE- AND TIME-DEPENDENT SLOWING DOWN IN HEAVY MEDIA

by

C. R. Weisbin
R. A. Forster
D. B. Smith

and

N. Corngold

ABSTRACT

To evaluate the potential of the lead slowing-down-time spectrometer quantitatively as a nuclear safeguards assay device, the time-, space-, and energy-dependent neutron diffusion equation has been solved for heavy moderators, and a FORTRAN-IV program, SLAHM (Slowing-Down Analysis in Heavy Moderators), was written to perform the required integrations.

Using this new calculational tool, spectral and spatial distributions have been obtained at a variety of times following introduction of a 14-MeV point source of neutrons into several different-sized lead assemblies. One can apparently achieve a $^{235}U/^{239}Pu$ discrimination ratio ≥ 5 with only limited self-shielding (even for high enrichment fuels) by examining the energy regions from 2.8 to 3.8 and 56 to 100 eV or, for highly enriched plutonium breeder fuel, 2.8 to 3.8 and 56 to 66 eV. Note that this technique requires a 2-m cube. Further, the neutron population for energies below the inelastic threshold based upon exponential attenuation ($e^{-B^2\tau}$) involving the neutron age (τ cm^2) must be estimated very carefully. The "true" age has been shown to be sensitive to both cross-section variation and the "free ride" afforded by the (n,2n) interaction.

I. INTRODUCTION

This report describes a solution to the full space-, time-, and energy-dependent neutron-diffusion equation and the application of that solution to a study of the relevance of the lead slowing-down-time spectrometer[1] to the United States' effort in the field of nuclear safeguards. The lead spectrometer requires a pulse of high-energy neutrons, typically 14 MeV, to be emitted near the center of a large cube of lead. After these neutrons undergo some rather complicated nonelastic processes in the initial slowing down phase, they gradually focus into an energy band that can be correlated analytically with the time elapsed since emission of the source pulse. By relating the time-dependent response of an unknown sample to the similar response of standard reference materials, one can determine the composition of the unknown sample quantitatively.

Previous experiments[2-4] have pointed out the difficulty in the discrimination of ^{239}Pu from ^{235}U, caused by resonance self-shielding at near-thermal energies. Proposals have therefore been made to apply the lead spectrometer at energies as high as the sub-MeV[5] region to eliminate this problem and to take advantage of the higher flux intensities. Careful consideration of the slowing down process is fundamental to the understanding and interpretation of the time-dependent response.

The prospect of calculating the neutronic properties of such a device appears straightforward at first, because age theory should hold well in such a large, heavy, nonabsorbing medium and the inelastic processes all take place within a short time. In fact, age theory does reasonably well if one has an accurate age value; however, such values are not readily available in the literature. Table I illustrates the sensitivity of the calculated neutron intensity at 3.5 eV using simple age theory by assuming several "effective" energies for the initiation of the elastic slowing down process. One observes that the relative neutron intensity calculated by means of age theory for a 1.3-m-diam sphere is almost a factor of 20 higher if the nonelastic processes yield an effective neutron source of 350-keV energy as compared to 1 MeV. This sensitivity is, of course, even more dramatic for smaller assemblies. From this example, it is clear that accurate computation of the neutron intensities requires careful consideration of the slowing down process. The neutron spectra and intensity below the inelastic threshold depend strongly on the treatment of nonelastic reactions which scatter neutrons to keV and lower energies.

TABLE I

SENSITIVITY OF NEUTRON AGE IN LEAD TO EFFECTIVE INITIAL ENERGY

Initial Energy (MeV)	Age to 100 eV (cm^2)	Age to 3.5 eV (cm^2)	Relative Intensity at 3.5 eV, 1.3-m Sphere
1.05	3593	4536	1.00
0.95	3492	4421	1.31
0.75	3250	4152	2.45
0.55	2927	3807	5.49
0.35	2433	3296	18.11

Detailed time-dependent neutronics calculations for heavy moderating materials also are not widespread in the literature. This is true for a number of reasons. Monte Carlo techniques are time-consuming because of the many collisions required per history. Multigrouping techniques are generally difficult because of the many groups required and the difficulties in choosing an appropriate time and energy matrix. Hence, previous calculations[5-7] have generally used a few broad energy groups, spatial variation in the normal mode (or none at all), and a rather crude treatment of elastic scattering.

The assumptions in this newer treatment include transport by diffusion theory and an age-theory expansion of the flux. Elastic scattering is assumed isotropic in the center-of-mass system, and cross sections are computed in a fine-group structure. Within these approximations, the solution to the differential equations is obtained in terms of integrals. The FORTRAN-IV program SLAHM (Slowing-Down Analysis in Heavy Moderators) was written to perform the required integrations. The region above the inelastic threshold is represented by ~10,000 groups (100 energy x 100 time bins). The spatial flux is expanded in orthogonal functions in either spherical, cylindrical, or rectangular geometry. Thus, the numerical solution is virtually independent of the number of space points of interest.

II. MATHEMATICAL DERIVATION

The Boltzmann equation describing neutron transport for nonfissionable materials can be written as

$$\nabla\cdot\underline{\Omega}N(\underline{r},\underline{\Omega},E,t) + \frac{1}{v}\frac{\partial N}{\partial t}(\underline{r},\underline{\Omega},E,t) + \Sigma_T(\underline{r},\underline{\Omega},E)N(\underline{r},\underline{\Omega},E,t)$$

$$= \int\int N(\underline{r},\underline{\Omega}',E',t)\Sigma_s(\underline{r},\underline{\Omega}'\rightarrow\underline{\Omega},E'\rightarrow E)dE'd\Omega' + S(\underline{r},\underline{\Omega},E,t) \quad . \tag{1}$$

∇	divergence vector (cm^{-1})
$\underline{\Omega}$	unit solid-angle vector (steradians)
$\underline{r}$	position of interest (cm)
t	time of interest (sec)
$n(\underline{r},\underline{\Omega},E,t)$	angular neutron density: number of neutrons at position $\underline{r}$ with energy E, going in direction $\underline{\Omega}$ at time t per unit volume, unit solid angle, and unit energy (neutrons/cm^3 - steradian - MeV)
v	neutron speed (cm/sec)
$N(\underline{r},\underline{\Omega},E,t)$	angular neutron flux = nv (neutrons/cm^2 - steradian - MeV - sec)
$\Sigma_T(\underline{r},\underline{\Omega},E)$	macroscopic total cross section at position $\underline{r}$ for neutrons of energy E going in direction $\underline{\Omega}$ (cm^{-1})
$\Sigma_s(\underline{r},\underline{\Omega}'\rightarrow\underline{\Omega},E'\rightarrow E)$	macroscopic differential-scattering cross section at position $\underline{r}$ for transferring neutrons with energy E' and direction $\underline{\Omega}'$ to energy E and direction $\underline{\Omega}$ per unit of final energy and solid angle (cm^{-1}/MeV - steradian)

$S(\underline{r},\Omega,E,t)$ external source of neutrons at position $\underline{r}$, energy E, direction Ω, and time t per unit of volume, energy, direction, and time (neutron/cm^3 - steradian - MeV - sec)

Equation (1) is integrated over all angles ($d\Omega$ ...) by assuming that the medium is isotropic for all processes; the angular dependence of the differential-scattering cross section is only a function of the dot product $(\Omega'\cdot\Omega)$.

$$\nabla\cdot J(\underline{r},E,t) + \frac{1}{v}\frac{\partial\phi}{\partial t}(\underline{r},E,t) + \Sigma_T(\underline{r},E)\phi(\underline{r},E,t)$$

$$= \int_{E'} \phi(\underline{r},E',t)\Sigma_s(\underline{r},E'\to E)dE' + s(\underline{r},E,t) \quad . \qquad (2)$$

The new quantities that appear are defined as:

$J(\underline{r},E,t)$ current vector = $\int N(\underline{r},\Omega,E,t)\Omega d\Omega$ (neutrons/cm^2 - MeV - sec)

$\phi(\underline{r},E,t)$ scalar flux = $\int N(\underline{r},\Omega,E,t)d\Omega$ (neutrons/cm^2 - MeV - sec)

$\Sigma_s(\underline{r},E'\to E)$ macroscopic differential-scattering cross section at space point $\underline{r}$ for scattering from E' to E = $\int\Sigma_s(\underline{r},E'\to E,\Omega'\cdot\Omega)d\Omega$ (cm^{-1}/MeV)

$s(\underline{r},E,t)$ external source = $\int S(\underline{r},\Omega,E,t)d\Omega$ (neutrons/cm^3 - MeV - sec)

III. DIFFUSION-THEORY APPROXIMATION

The removal term is divided into a sum of elastic and nonelastic components, and the scattering integral is represented explicitly as the sum of contributions from elastic, discrete-inelastic, and continuum interactions.[8] Diffusion theory is reasonable because most of the neutrons are quickly (less than 1 μsec) degraded to energies below which there is little absorption and thus are not expected to have migrated far from the source. Neutrons of these lower energies are essentially diffusing elastically in a rather large system.

Converting the variable of interest to neutron density per unit of velocity and applying Ficks' law, one obtains the following form of the diffusion equation from Eq. (2)

$$-\frac{v\nabla^2 n(\underline{r},v,t)}{3\Sigma_{tr}(\underline{r},v)} + \frac{\partial n}{\partial t}(\underline{r},v,t) + v\Sigma_{ne}(\underline{r},v)n(\underline{r},v,t)$$

$$= \int v'n(\underline{r},v',t)\Sigma_{el}(\underline{r},v'\to v)dv' + S_1(\underline{r},v,t)$$

$$+ S_2(\underline{r},v,t) - v\Sigma_{el}(\underline{r},v)n(\underline{r},v,t) + s(\underline{r},v,t) \quad . \qquad (3)$$

The discrete inelastic and continuum integrals have been denoted by S_1 and S_2, respectively. Other quantities defined in Eq. (3) include

$n(\underline{r},v,t)$ neutron density/velocity at time t (n/cm^3-cm/sec)

$\Sigma_{tr}(\underline{r},v)$ macroscopic transport cross section (= 1/3D where D is the diffusion coefficient) (cm^{-1})

$\Sigma_{el}(\underline{r},v)$ macroscopic elastic-scattering cross section (cm^{-1})

$\Sigma_{ne}(\underline{r},v)$ macroscopic nonelastic cross section (cm^{-1})

$s(\underline{r},v,t)$ external source/velocity (n/cm^3-cm/sec-sec)

IV. AGE EXPANSION

The facts that the moderator is a heavy material and that the flux spectrum is expected to approach 1/E asymptotically suggest that one expand $n(\underline{r},v',t)v'^2$ about $n(\underline{r},v,t)v^2$ in a two-term Taylor series to evaluate the scattering integral. If one now assumes that elastic scattering is isotropic in the center of mass and constant within the range of an elastic integral, the first of the terms from the scattering integral just cancels the removal term owing to elastic scattering, and one obtains

$$-\frac{v\nabla^2 n(\underline{r},v,t)}{3\Sigma_{tr}(\underline{r},v)} + \frac{\partial n}{\partial t}(\underline{r},v,t) + v\Sigma_{ne}(\underline{r},v)n(\underline{r},v,t)$$

$$= \frac{\Sigma_{el}(\underline{r},v)}{A}\frac{\partial}{\partial v}[n(\underline{r},v,t)v^2] + S_1(\underline{r},v,t)$$

$$+ S_2(\underline{r},v,t) + s(\underline{r},v,t) \quad . \qquad (4)$$

In Eq. (4), the derivative term with respect to v is multiplied by 1/A, a very small number. However, the mathematical form of the equation is very different if this term is not present.

V. ORTHOGONAL FUNCTION EXPANSION

The neutron density is expanded into a set of orthogonal functions $f_K(r)$. (Recall that $\underline{r}$ stands for [x,y,z] or [r,θ,φ].)

$$n(\underline{r},v,t) = \sum_K f_K(\underline{r}) n_K(v,t) \quad , \tag{5}$$

where the $f_K(\underline{r})$ are orthonormal solutions to the Helmholtz equation

$$\nabla^2 f_K(\underline{r}) + B_K^2 f_K(\underline{r}) = 0 \quad , \tag{6}$$

with the boundary condition $f_K(r_s) = 0$, r_s being a point on the surface and $\int f_K(\underline{r}) f_L(\underline{r}) dV = \delta_{KL}$.

The external source and discrete-inelastic and continuum integrals are similarly expanded. This requires a homogeneous medium within the boundary so that macroscopic cross sections can be taken as independent of position. The external source is located at the center of the moderating assembly, with one neutron emitted isotropically in the lab system at time t_o with energy E_o. Implementing the above conditions, we have

$$s(\underline{r},v,t) = \sum_K f_K(\underline{r}) s_K(v,t) \quad , \tag{7}$$

$$S_1(\underline{r},v,t) = \sum_K f_K(\underline{r}) S_1^K(v,t) \quad , \tag{8}$$

$$S_2(\underline{r},v,t) = \sum_K f_K(\underline{r}) S_2^K(v,t) \quad , \tag{9}$$

$$s_K(v,t) = \int \frac{\delta(\underline{r}-r_o)}{4\pi r^2} \delta(v-v_o)\delta(t-t_o) f_K(\underline{r}) dV$$

$$= \delta(v-v_o)\delta(t-t_o) f_K(r_o) \quad . \tag{10}$$

VI. ELASTIC SCATTERING ONLY

Consider first the energy region $E > E_o - \theta$ where E_o is the source energy and θ is the energy of the lowest excited level. In this case, the only scattering contribution is from elastic scattering, and one obtains

$$\frac{v}{3\Sigma_{tr}(v)} n_K(v,t) B_K^2 + \frac{\partial}{\partial t} n_K(v,t) + v\Sigma_{ne}(v) n_K(v,t)$$

$$= -\frac{\Sigma_{el}(v)}{A} \frac{\partial}{\partial v} [n_K(v,t) v^2] + \delta(v-v_o)\delta(t-t_o) f_K(r_o) \quad . \tag{11}$$

VII. METHOD OF SOLUTION

Equation (11) is solved by taking Laplace transforms of the time variable, thus reducing Eq. (11) to a speed-dependent linear differential equation that can be solved directly. This solution is then inverted to reconstruct the time dependence for each of the spatial harmonics. The final solution is obtained by synthesizing each of the spatial modes according to Eq. (5). Cross-section variation is simulated by a histogram (with many bins), and a boundary condition is applied numerically to account for discontinuities caused by the histogram simulation.

Define the Laplace transform,

$$\tilde{n}_K(v,\lambda) = \int_o^\infty dt e^{-\lambda t} n_K(v,t) \quad , \tag{12}$$

and apply the operator $\int_o^\infty dt\, e^{-\lambda t} \ldots$ to Eq. (11) to obtain

$$\frac{\partial}{\partial v}\left[\tilde{n}_K(v,\lambda) v^2\right] - \frac{A}{\Sigma_{el}(v)}\left(\frac{B_K^2}{3\Sigma_{tr}(v)} + \frac{\lambda}{v^2} + \frac{\Sigma_{ne}(v)}{v}\right)$$

$$\times v^2 \tilde{n}_K(v,\lambda) = 0 \quad , \tag{13}$$

for $t > t_o$, $v < v_o$. For a particular energy interval, the group-averaged cross section may be taken as constant.

VIII. BOUNDARY CONDITION

For the highest energy group, the applicable boundary condition can be derived by going back to the transformed equation

$$\frac{\Sigma_{el}}{A} \frac{\partial}{\partial v}\left[\tilde{n}_K(v,\lambda) v^2\right] + \delta(v-v_o) e^{-\lambda t_o} f_K(r_o)$$

$$= \frac{v}{3\Sigma_{tr}} \tilde{n}_K(v,\lambda) B_K^2 + v\Sigma_{ne}\tilde{n}_K(v,\lambda) + \lambda \tilde{n}_K(v,\lambda) \quad , \tag{14}$$

and integrating from $v = v_o - \varepsilon$ to $v = v_o + \varepsilon$ where v_o is the highest speed in the problem and epsilon is infinitesmally small. One finds

$$\tilde{n}_K(v_o,\lambda) = \frac{A e^{-\lambda t_o} f_K(r_o)}{v_o^2 \Sigma_{el}} \quad . \tag{15}$$

For any other group, the boundary condition is obtained by integrating Eq. (14) from $v = v_B - \varepsilon \equiv v_{B-}$ to $v = v_B + \varepsilon \equiv v_{B+}$ where v_B is the lower velocity

bound of group B. In the limit as ε approaches zero, this reduces to

$$\tilde{n}_K(v_{B-},\lambda) = \tilde{n}_K(v_{B+},\lambda) \quad ; \tag{16}$$

i.e., the neutron density at some energy boundary B as determined from the solutions in groups above and below the boundary (which may, of course, have different cross sections) must be equal. For the top group, the solution to Eq. (14) is given by

$$\tilde{n}_K(v,\lambda) = \frac{1}{v^2}\frac{f_K(r_o)A}{\Sigma_{el}} e^{\frac{\lambda A}{\Sigma_{el}}\left(\frac{1}{v_o}-\frac{1}{v}-\frac{t_o\Sigma_{el}}{A}\right)} \times \left(\frac{v}{v_o}\right)^{\left(\frac{AB_K^2}{3\Sigma_{el}\Sigma_{tr}}+\frac{A\Sigma_{ne}}{\Sigma_{el}}\right)} . \tag{17}$$

The form of the solution for lower-energy groups (still elastic scattering only) is similar to Eq. (17) modified by a coefficient $F_K(v)$ resulting from application of Eq. (16) at each preceding boundary. $F_K(v)$ can be written as

$$F_K(v) = \prod_{\ell=1}^{j-1}\left(\frac{v_\ell}{v_o}\right)^{\left(C_\ell - C_{\ell+1}\right)} , \tag{18}$$

where

$$C_\ell = \frac{AB_K^2}{3\Sigma_{el}^\ell\Sigma_{tr}^\ell} + \frac{A\Sigma_{ne}^\ell}{\Sigma_{el}^\ell} .$$

Σ_{el}^ℓ = macroscopic total elastic cross section of energy group ℓ bounded by speeds v_ℓ and $v_{\ell-1}$.

v_ℓ = lower velocity boundary of group ℓ; j is the group containing v $\left(v_\ell > v_{\ell+1}\right)$.

As expected, for the case of constant cross section, $F_K(v) = 1$ and boundary conditions do not affect the solution.

Furthermore, the time-dependent term in Eq. (17) is generalized to

$$e^{\lambda A\left\{\left[\sum_{\ell=1}^{j-1}\frac{1}{\Sigma_{el}^\ell}\left(\frac{1}{v_{\ell-1}}-\frac{1}{v_\ell}\right)\right]+\frac{1}{\Sigma_{el}^j}\left(\frac{1}{v_{j-1}}-\frac{1}{v}\right)-\frac{t_o\Sigma_{el}^j}{A}\right\}} , \tag{19}$$

so that, in general, Eq. (17) becomes

$$\tilde{n}_K(v,\lambda) = \frac{F_K(v)f_K(r_o)A}{v^2\Sigma_{el}^j} \times e^{\lambda A\left\{\left[\sum_{\ell=1}^{j-1}\frac{1}{\Sigma_{el}^\ell}\left(\frac{1}{v_{\ell-1}}-\frac{1}{v_\ell}\right)\right]+\frac{1}{\Sigma_{el}^j}\left(\frac{1}{v_{j-1}}-\frac{1}{v}\right)-\frac{t_o\Sigma_{el}^j}{A}\right\}} \times \left(\frac{v}{v_o}\right)^{\left(\frac{AB_K^2}{3\Sigma_{el}^j\Sigma_{tr}^j}+\frac{A\Sigma_{ne}^j}{\Sigma_{el}^j}\right)} . \tag{20}$$

IX. TIME INVERSION

One next inverts Eq. (20) to regain the functional dependence of the time variable. Define

$$M(v) \equiv A\left\{\left[\sum_{\ell=1}^{j-1}\frac{1}{\Sigma_{el}^\ell}\left(\frac{1}{v_\ell}-\frac{1}{v_{\ell-1}}\right)\right]+\frac{1}{\Sigma_{el}^j}\left(\frac{1}{v}-\frac{1}{v_{j-1}}\right)+\frac{t_o\Sigma_{el}^j}{A}\right\} . \tag{21}$$

The time dependence of Eq. (20) is now contained solely in the term $e^{-\lambda M(v)}$. Recall that

$$\int_0^\infty dt\, e^{-\lambda t}\delta(t-c) = e^{-\lambda c} \text{ if c is a positive constant} = 0 \text{ otherwise} . \tag{22}$$

Then, for elastic scattering only

$$\tilde{n}_K(v,t) = \frac{F_K(v)f_K(r_o)A}{v^2\Sigma_{el}^j}\delta[t-M(v)]\left(\frac{v}{v_o}\right)^{\left(\frac{AB_K^2}{3\Sigma_{el}^j\Sigma_{tr}^j}+\frac{A\Sigma_{ne}^j}{\Sigma_{el}^j}\right)} , \tag{23}$$

and the solution to Eq. (11), for elastic scattering only, can be written as

$$n(\underline{r},v,t) = \frac{A}{v^2\Sigma_{el}^j}\delta[t-M(v)] \times \sum_K f_K(\underline{r})f_K(r_o)F_K(v)\left(\frac{v}{v_o}\right)^{\left(\frac{AB_K^2}{3\Sigma_{el}^j\Sigma_{tr}^j}+\frac{A\Sigma_{ne}^j}{\Sigma_{el}^j}\right)} . \tag{24}$$

X. EXTENSION TO INCLUDE DISCRETE INELASTIC AND (n,2n) REACTIONS

The solutions for the energy regions below $E_o-\theta$, including discrete inelastic and continuum contributions, are obtained in an analogous fashion. The differential equation in speed is now, however, inhomogeneous with respect to source terms containing inelastic and (n,2n) reactions followed by elastic slowing down.

The final solution including all contributions is given below. Level interactions have been assumed to take place with an infinitely heavy target, and nonelastic reactions are assumed to occur instantaneously. This solution is obtained from the inhomogeneous equation using the variation-of-parameters technique. The result is

$$
\begin{aligned}
n(\underline{r},v,t) = {} & \frac{A}{v^2\Sigma_{el}^j}\,\delta[t-M(v)]\sum_K f_K(\underline{r})f_K(r_o)F_K(v) \\
& \times\left(\frac{v}{v_o}\right)^{\left(\frac{AB_K^2}{3\Sigma_{el}^j\Sigma_{tr}^j}+\frac{A\Sigma_{ne}^j}{\Sigma_{el}^j}\right)} + \frac{A}{v^2\Sigma_{el}^j}\sum_K f_K(\underline{r})G_K(v) \\
& \times\left(\frac{v}{v_o}\right)^{\left(\frac{AB_K^2}{3\Sigma_{el}^j\Sigma_{tr}^j}+\frac{A\Sigma_{ne}^j}{\Sigma_{el}^j}\right)}\sum_{\text{levels}}\int_v^{v_o} v'(v'',\theta)\Sigma_i^\theta[v'(v'',\theta)] \\
& \times n_K\{v'(v'',\theta),t-[M(v)-M(v'')]\}\left(\frac{v_o}{v''}\right)^{\left(\frac{AB_K^2}{3\Sigma_{el}^j\Sigma_{tr}^j}+\frac{A\Sigma_{ne}^j}{\Sigma_{el}^j}\right)}dv'' \\
& + \frac{A}{v^2\Sigma_{el}^j}\sum_K f_K(\underline{r})H_K(v)\left(\frac{v}{v_o}\right)^{\left(\frac{AB_K^2}{3\Sigma_{el}^j\Sigma_{tr}^j}+\frac{A\Sigma_{ne}^j}{\Sigma_{el}^j}\right)} \\
& \times\int_{v_{2n}\text{ or }v}^{v_o}\int_v^{v'}\left(\frac{v_o}{v''}\right)^{\left(\frac{AB_K^2}{3\Sigma_{el}^j\Sigma_{tr}^j}+\frac{A\Sigma_{ne}^j}{\Sigma_{el}^j}\right)} \\
& \times n_K\{v',t-[M(v)-M(v'')]\}\Sigma_{2n}(v'\to v'')dv''dv' \quad ,
\end{aligned}
\tag{25}
$$

where $\Sigma_i^\theta[v'(v'',\theta)]$ is the inelastic cross section at speed v' for exciting level θ, and the neutron emerges from the reaction with speed v" and slows down elastically to speed v. $\Sigma_{2n}(v'\to v'')$ is the macroscopic differential (n,2n) cross section at v' for scattering to v". $G_K(v)$ and $H_K(v)$ are the terms resulting from application of the boundary condition, Eq. (16), and are rather complicated functions. None of the three functions $F_K(v)$, $G_K(v)$, or $H_K(v)$ is used explicitly in SLAHM. Instead, Eq. (16) is satisfied numerically at each velocity boundary v_B.

The three terms in Eq. (25) are easily interpreted. The first is simply those neutrons reaching v directly from the source by elastic scattering only. The second term includes those neutrons whose last nonelastic scattering collision (before reaching v) was a discrete inelastic scattering, and the third term comprises those neutrons whose last nonelastic transfer was by an (n,2n) collision. The (n,2n) process scatters neutrons from v' to v" where they begin to slow down elastically to v. Because both the initial speed v' and the final speed v" are variables, the double integral results.

XI. NUMERICAL CONSIDERATIONS

Equation (25) is solved, one group at a time, starting with the highest energy group and proceeding stepwise downward to the group that includes the lowest-lying level for lead (~570 keV). Each flux computed in this energy range is stored for later use as an effective source for computation of the flux at lower energies. Neutrons below 570 keV can only slow down to energies of interest by means of elastic scattering for which an analytical expression is available. Therefore one can compute the neutron intensity at any energy of interest directly using only information related to the superthreshold neutron flux as a function of energy and time. For example, to compute the neutron intensity at 100 eV, it is only necessary to store the flux dependence above 570 keV; one need not compute the flux at 200 eV.

The problem of slowing down in lead is quite analogous to the deep-penetration problem in shielding. In the latter case, one is concerned primarily with the few neutrons that are able to traverse many mean free paths. These neutrons typically get "free rides" through windows in the total cross

section, so it is important to consider these cross section features carefully. Slowing down in lead is a deep-penetration problem in the energy variable instead of the spatial variable. Neutrons generally undergo many collisions and leak from the system before being degraded appreciably in energy. Only those neutrons that receive a "free ride" by (n,2n) or discrete-inelastic interactions manage to slow down to lower energies before escaping from the system. Hence, it is important to consider these reactions carefully. Orders of magnitude discrepancies have been observed in the extreme case of totally neglecting level interactions.

XII. COMPARISON OF SLAHM WITH KNOWN ANALYTIC AND EXPERIMENTAL RESULTS

The numerical results obtained from SLAHM in the simple case of energy-dependent elastic scattering plus a single level of discrete inelastic scattering have been compared and agree well with the known analytic solution. In addition, Bergman's experimental work reported at the 1955 Geneva Conference has been modeled. He reports a counting rate of 250 cpm for 100-eV neutrons at the center of a 2-m lead pile. A count rate of 303 cpm was computed using SLAHM. Thus, with reasonable confidence* in the ability to compute and understand the slowing down processes, one next considers some of the practical applications such as the ability to determine quantitatively the amount of ^{239}Pu and ^{235}U contained in mixed-oxide reactor fuel pins.

XIII. APPLICATION OF THE LEAD SLOWING-DOWN-TIME SPECTROMETER (LSDTS) TECHNIQUES TO SAFEGUARDS PROBLEMS

To differentiate between ^{239}Pu and ^{235}U using the LSDTS technique, irradiations in at least two energy intervals are required in order to obtain two equations for two unknowns.

A review of the barn book[9] suggests one region that may be applicable; this is the region from 1.5 to 6.5 eV shown in Fig. 1. The data for Fig. 1 were taken from the 1968 KFK-750 report.[10] One is bound on the left by the well-known ^{240}Pu resonance at 1 eV, and on the right by the 6.67-eV ^{238}U resonance and the 7.8 eV resonance of ^{239}Pu. However, within the 2- to 6-eV region, the cross sections

*Admittedly, the number of checks performed was limited, and more work must be done in this area.

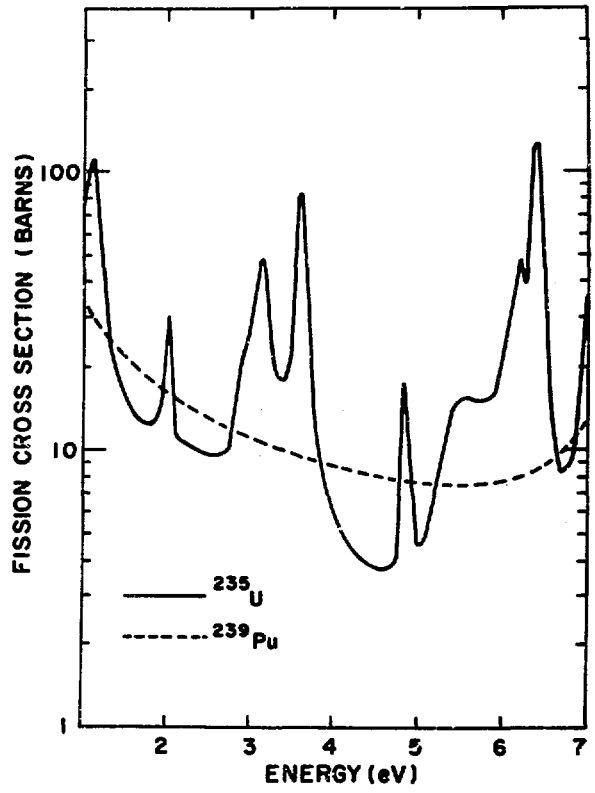

Fig. 1. ^{235}U and ^{239}Pu fission cross sections, 1- to 7-eV energy.

are small enough not to present any self-shielding problems of practical importance. If the count rate is sufficient, this appears to be an interesting possibility.

With respect to count-rate considerations, note Table II which illustrates the sensitivity of the neutron intensity per unit volume to the dimensions of the pile. A substantial increase in intensity can be achieved by going to larger cubes, particularly when considering lower energies (eV region). The dilution of the neutrons in the larger volume is more than compensated for by the reduced leakage. Lead cubes of about two meters on a side should be sufficient to measure the prompt-fission neutrons induced in the 1.5- to 6.5-eV region and provide meaningful statistics.

TABLE II

SENSITIVITY OF NEUTRON INTENSITY PER VOLUME TO LEAD PILE DIMENSIONS

Energy (ev)	Sphere Radius (cm) 50	65	100
3.5	1.	244	12,900
100.0	1.	64	1,100

The 2.8- to 3.8-eV energy region is depicted in Fig. 2. It is characterized by an ∿30-μsec time interval and yields a $^{235}U/^{239}Pu$ discrimination ratio of ∿2.5 without any interfering resonance from ^{238}U or higher isotopes of plutonium.

A second energy region of interest is that from 56 to 100 eV shown in Fig. 3. Data for this figure were taken from Lemley's recent measurements.[11] Earlier German work by Baumung et al.[12] examined the region from 60 to 120 eV. We recommend here that the additional 2 μsec corresponding to 56 to 66 eV be included because the plutonium cross section is higher than the ^{235}U cross section by about a factor of three and the fissions induced will be a significant part (∿14%) of the total. Conversely, the range from 100 to 120 eV, where the $^{239}Pu/^{235}U$ discrimination capability is appreciably lower, was not included. Note that cross sections in the 56- to 100-eV region are substantially higher, and self-shielding corrections up to ∿30% could be introduced, depending upon the fuel composition. If the plutonium concentration is known, a priori, to be that high, a more satisfactory approach is indicated in Fig. 4 which suggests that one focus attention on the more restricted 56- to 66-eV range. This is a more difficult experiment because the counting time involved is ∿3 to 4 μsec so the source pulse width must be confined to less than 1 μsec. However, such an approach effectively eliminates the self-shielding

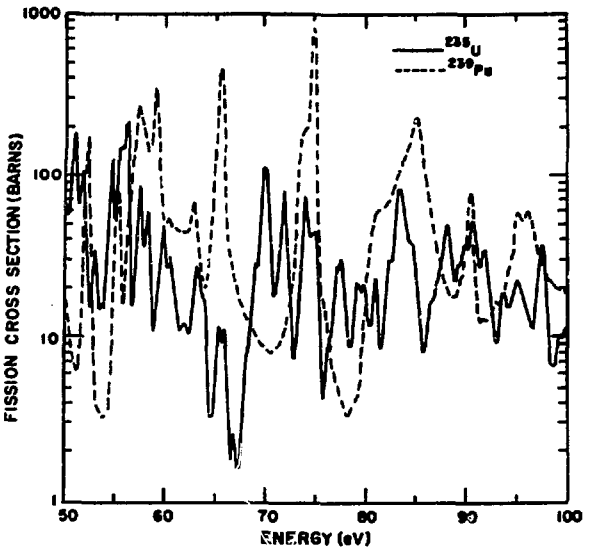

Fig. 3. ^{235}U and ^{239}Pu fission cross sections 56- to 100-eV energy.

problems by entirely avoiding the 75-eV resonance of ^{239}Pu; the count-rate loss due to diminished source intensity and counting time is more than compensated by the factor of ten increase in ^{239}Pu concentration in fast-reactor fuels.

To sum up, we propose application of the LSDTS technique using a 2-m^3 lead pile with investigation of the 2.8- to 3.8- and 56- to 100-eV energy ranges, or for fast-breeder, high-plutonium-concentration pins, the 2.8- to 3.8- and 56- to 66-eV ranges.

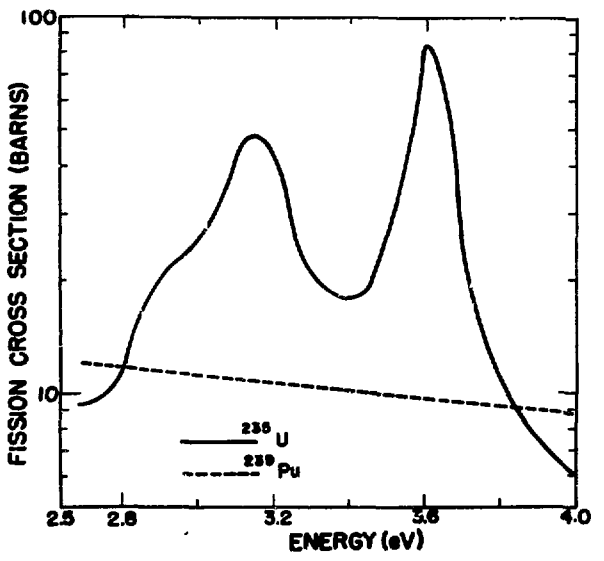

Fig. 2. ^{235}U and ^{239}Pu fission cross sections, 2.8- to 3.8-eV energy.

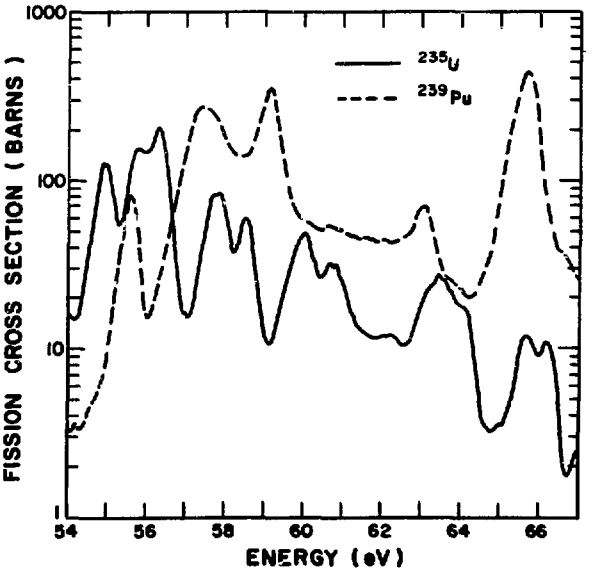

Fig. 4. ^{235}U and ^{239}Pu fission cross sections, 54- to 67-eV energy.

The net discrimination

$$D = \left(\frac{\text{counts } ^{235}U}{\text{counts } ^{239}Pu}\right)_{2.8 \text{ to } 3.8 \text{ eV}} \times \left(\frac{\text{counts } ^{239}Pu}{\text{counts } ^{235}U}\right)_{56 \text{ to } 100 \text{ eV}}$$

achieved in approximately five. Table III presents estimates of counting rates for these regions using the results obtained from SLAHM. These counting rates were obtained assuming a 2 x 10^8 n/sec source of 14-MeV neutrons, 1-m-long fuel pins, ∿1 cm in diameter, and 0.2% detector efficiency.

TABLE III

EXPECTED COUNT RATE IN A 2-m-DIAM LEAD SPHERE AS A FUNCTION OF FUEL COMPOSITION[a]

Fuel Composition (%)		Average Count Rate (56 to 100 eV) (cpm)	Average Count Rate (2.8 to 3.8 eV) (cpm)
^{235}U	2.5	1,500	540
^{239}Pu	0.5		
^{235}U	0.5	23,000	1,300
^{239}Pu	20.0		
^{235}U	8.0	12,000	2,200
^{239}Pu	8.0		

[a]Cockcroft-Walton source of 2 x 10^8 n/sec.

XIV. CONCLUSIONS

1. There are two natural energy ranges (2.8 to 3.8 and 56 to 100 eV) that together provide a discrimination factor of 5 between ^{239}Pu and ^{235}U with little problem of self-shielding induced by these two isotopes.

2. For typical fast-breeder fuel compositions, the application of the LSDTS technique using a 2-m-diam lead sphere involves assay times of <10 min for 1% counting statistics.

3. Our analysis of the slowing down process has provided a technique by which to compute the appropriate subthreshold (for inelastic processes) source for neutron slowing down in lead.

4. The effective age of 14-MeV neutrons in lead has been shown to be very sensitive to the "effective" initial spectrum as shown in Table I.

REFERENCES

1. A. A. Bergman, A. I. Isakov, I. D. Gurin, F. L. Shapiro, I. V. Shtranikh, and M. V. Kazarnovski, "A Neutron Spectrometer Based on Measuring the Slowing-Down Time of Neutrons in Lead," Proc. Intern. Conf. Peaceful Uses At. Energy, Geneva, 1955, P/642, Vol. IV, pp. 135-146 (1955).

2. H. Krinninger, S. Wiesner, and C. Faber, "Pulsed Neutron Method for Nondestructive and Simultaneous Determination of the ^{235}U and ^{239}Pu Contents of Irradiated and Non-Irradiated Reactor Fuel Elements," Nucl. Instr. Meth., 73 13 (1969).

3. D. Stegamann and H. Seufert, "Application of the Slowing Down Time Spectrometer for the Control of Fissionable Material," Trans. Am. Nucl. Soc., 11, 658 (1968).

4. M. P. Navalkar, K. Chandramoleshwar, and D. V. S. Ramakrishna, "A Feasibility Study of Non-destructive Assay of ^{239}Pu and ^{235}U in Irradiated Samples Using a Slowing Down Lead Spectrometer," Nukleonik, 11, 54 (1968).

5. R. L. Bramblett, R. O. Ginaven, T. Gozani, A. T. Hyde, L. A. Kull, J. I. McMillan, D. E. Rundquist, and G. D. Trimble, "Application of Photoinduced Reactions to Nuclear Materials Safeguards Problems," GA-10272, pp. 77-85, Gulf Radiation Technology (1970).

6. T. J. Williamson and R. W. Albrecht, "Calculations of Neutron Time-Energy Distributions in Heavy Moderators," Nucl. Sci. Eng., 42, 97 (1970).

7. J. R. Beyster, "The Application of the Slowing Down Spectrometer to Nuclear Materials Assay," BNL-50232, Brookhaven National Laboratory (1970).

8. B. R. S. Buckingham, K. Parker, and E. D. Pendlebury, "Neutron Cross Sections of Selected Elements and Isotopes for Use in Neutronic Calculations in the Energy Range .025 eV-15 MeV," AWRE-O-28/60, Atomic Weapons Research Establishment, Aldermaston, England (1961).

9. John R. Stehn, Murrey D. Goldberg, Renate Wiener-Chasman, Said F. Mughabghab, Benjamin A. Magurno, and Victoria M. May, "Neutron Cross Sections," BNL-325, Vol. III, Brookhaven National Laboratory (1965).

10. I. Langner, J. J. Schmidt, and D. Woll, "Tables of Evaluated Neutron Cross Sections for Fast Reactor Materials," KFK 750, Institute Für Neutronenphysik und Reaktortechnik, Karlsruhe, Germany (1968).

11. J. R. Lemley, G. A. Keyworth, and B. C. Diven, "High Resolution Fission Cross Section of Uranium-235 from 20 eV to 100 keV," Nucl. Sci. Eng., 43, (1971).

12. K. Baumung, K. Böhnel, J. Klunker, M. Küchle, and J. Wolff, "Investigations into Non-Destructive Safeguards Techniques," in Safeguards Techniques, Proceedings of a Symposium in Karlsruhe, July 6-10, 1970, IAEA-SM-133/90, Vol. II, pp. 177-192.